Landscape and Urban Planning 185 (2019) 127–140

Contents lists available at ScienceDirect

Landscape and Urban Planning

journal homepage: www.elsevier.com/locate/landurbplan

Research Paper

Scale dependence of the benefits and efficiency of green and cool roofs

Jiachuan Yang[a,b,*], Elie Bou-Zeid[a]

[a] Department of Civil and Environmental Engineering, Princeton University, Princeton, NJ 08544, United States
[b] Department of Civil and Environmental Engineering, The Hong Kong University of Science and Technology, Kowloon, Hong Kong

ARTICLE INFO

Keywords:
Cool roof
Cooling efficiency
Green roof
Heat island mitigation
Urban planning

ABSTRACT

Cool and green roofs are widely adopted measures for curtailing summertime urban heat islands. Existing numerical studies to assess their effectiveness and cooling benefits usually assume an unrealistic 100% coverage across the entire metropolis. This study investigates the scale dependence of the absolute cooling benefits and efficiency (cooling per adapted roof area) of cool and green roofs in a typical summer when they are installed over 25% of building rooftops at local, city, or regional scales. Six major U.S. cities with active climate action plans in different geoclimatic zones are compared through high-resolution simulations using the Weather Research and Forecasting model. The results reveal that reductions in 2-m air temperature over the urban core increase non-linearly with the intervention area, and the benefits of both roof types scale similarly. This scale-dependence of urban core cooling is not universal, but is rather controlled by the shape of metropolitan areas and wind pattern. The siting of mitigation measures hence plays an important role especially under windy conditions, and some urban cores are not able to achieve a noticeable and consistent cooling by retrofitting their own rooftops. Regional-scale deployments of mitigation strategies, on the other hand, yield a more substantial temperature reduction but with a lower efficiency. The scale-dependence of regional cooling efficiency showed remarkable similarity across studied cities, yielding a potentially generalizable power law. The successful resiliency plans for cities should account for the scale dependence and geoclimatic determinants of the achievable cooling, and identify the target neighborhoods of most interest.

1. Introduction

The urban heat island (UHI), a phenomenon whereby urban areas experience higher temperatures than the rural areas that surround them, is one of the most evident human modification of the natural environment (Oke, 1982). Elevated temperatures in cities have adverse implications for energy demand, water resources, and resident health, particularly at night during hot periods (Grimm et al., 2008; Grimmond, 2007). The challenges they pose will continue to grow with future climate change (Intergovernmental Panel on Climate Change, 2014). As such, heat islands are widely recognized as stumbling blocks in the sustainable pathways of metropolitan areas, and recent years have seen substantial resources dedicated to investigating and implementing UHI mitigation strategies (Gartland, 2012; Rizwan, Dennis, & Chunho, 2008). The proposed strategies that are most studied in the literature and adopted by cities are the use of high-albedo materials and green infrastructure (Norton et al., 2015; Ramamurthy, Sun, Rule, & Bou-Zeid, 2015; Santamouris, 2014). Because urban land is highly valuable, and because highly-reflective materials could degrade outdoor human thermal comfort when applied at ground level by reflecting radiation towards pedestrians (Yang, Wang, Kaloush, & Dylla, 2016), strategies focusing on building rooftops have been increasingly promoted to create cooling spaces. Cool roofs use high-albedo materials to reduce urban temperatures by increasing the reflection of incoming solar radiation, while green roofs adopt vegetation to cool the built environment via evapotranspiration. In addition, green roofs can generate other ecosystem services including storm water retention, aesthetic improvement, habitat provision, food production, and air pollutant removal (Carter & Fowler, 2008).

Field experiments at various locations around the world show that the daily maximum surface temperature of cool and green roofs can be 10–30 °C lower than that of conventional roofs (Santamouris, 2013; Takebayashi & Moriyama, 2007; Yang, Wang, & Kaloush, 2015). Reduced surface temperature and diurnal temperature variation reduce the direct heating of outdoor air; in addition, they can substantially moderate building heat gain and increase energy efficiency in the summer (Parizotto & Lamberts, 2011; Shen, Tan, & Tzempelikos, 2011). Consequently, waste heat release from air conditioning systems during the summer, which contributes more than 1 °C to UHIs in some urban locations (de Munck et al., 2013; Salamanca, Georgescu, Mahalov,

* Corresponding author at: The Hong Kong University of Science and Technology, Kowloon, Hong Kong.
E-mail address: cejcyang@ust.hk (J. Yang).

https://doi.org/10.1016/j.landurbplan.2019.02.004
Received 1 March 2018; Received in revised form 1 February 2019; Accepted 2 February 2019

Moustaoui, & Wang, 2014), can be reduced to provide further urban cooling. Building-to-block scale numerical simulations reported benefits consistent with the in-situ measurements (Ramamurthy et al., 2015; Sailor, Elley, & Gibson, 2012; Yang, Wang, Kaloush et al., 2016; Zinzi & Agnoli, 2012).

While these interventions at a single site can rely on both measurements and models, the wider benefits to the whole city and the decrease in air temperature can only be evaluated through simulations because no urban region has yet achieved a sufficiently extensive intervention to have a measurable influence beyond the building scale. Thus, at city and regional scales, the cooling effect of cool and green roofs has been investigated through climate models that, ideally, can account for landscape heterogeneity and land-atmosphere interactions (Millstein & Menon, 2011; Yang & Wang, 2017). Improved parameterizations of the urban land surface in climate models have produced more accurate simulations of the climatic impact of cool and green roofs in recent years (Li, Bou-Zeid, & Oppenheimer, 2014; Wang, Bou-Zeid, & Smith, 2013; Yang, Wang, & Chen et al., 2015). Nevertheless, numerical experiments tend to focus on the maximum potential benefit of mitigation strategies, that is, on 100% coverage uniformly over the entire metropolitan area (Georgescu, Morefield, Bierwagen, & Weaver, 2014; Sharma et al., 2016). Li et al. (2014) was the first study to consider a smaller fraction of roofs to be converted to cool or green (down to only 10% of roofs), but they still assumed implementation over the whole metropolitan region and have only considered one city (Baltimore, MD). They reported that a regional-scale deployment of green or cool roofs over 30% of urban rooftops induces a maximum reduction in 2-m air temperature of less than 0.2 °C (across the diurnal temperature cycle averaged over 4 days).

Such modelling results are at present the best available resource to guide urban planning and policy in the context of long-term environmental adaptation, but they remain insufficient. For example, although many cities have initiated plans of implementing cool and green roofs (Carter & Fowler, 2008), up till now such efforts appear to cover a limited extent that is far below the coverage these modelling studies investigate. For example, from 1995 to 2008, the implementation of cool roofs has increased Chicago's average albedo by only 0.016, while the installation of green roofs has increased Chicago's vegetated surfaces by a mere 9.4 km^2 (Mackey, Lee, & Smith, 2012). In addition, mitigation policies are designed on a city-by-city basis and vary extensively in scope and ambition (Reckien et al., 2014); consequently, assuming a uniform distribution at the regional scale is quite reductionist. In reality, due to the difference in land use function, economic activity, perception of environmental challenges, and government structure and jurisdictions, executions of mitigation strategies may diverge considerably among districts and communities at the sub-city scale, as well as over the larger metropolitan areas. New York City is a good illustration since the actual metropolitan area spans the city's five boroughs, as well as counties in New Jersey, Connecticut, and New York states. Mitigation plans can thus be implemented by the city for its dense urban core (Manhattan), for the whole city (all boroughs), or in cooperation with surrounding counties for the whole metropolitan area. One resulting important question for heat island mitigation strategies is thus: how do the cooling benefits from a given intervention vary with its spatial extent?

Remote sensing studies found that land surface temperatures are closely related to vegetation fraction (Jin & Dickinson, 2010). Land surface temperature decreases by about 0.86 °C when green space cover increases by 10% (Li, Zhou, Ouyang, Xu, & Zheng, 2012). A recent meta-analysis reported that urban park surfaces, on average, are 0.94 °C cooler in the day than surrounding urban surfaces (Bowler, Buyung-Ali, Knight, & Pullin, 2010). However, the spatial configuration of these cooler surfaces plays an important role in regulating local air temperature (Maimaitiyiming et al., 2014), and urban vegetation is not effective if it does not span a sufficiently large footprint (e.g., ~500–1000 m, Wang, Fan, Myint, & Wang, 2016). This confirms that whether the cooling benefits of cool and green roofs will match the expectation of cities' heat island mitigation plans depends on the spatial extent and siting of the mitigation efforts. While this is understood qualitatively, what remains unknown are the quantitative scaling laws of cooling benefits with the intervention's spatial scale. Moreover, many studies have reported a negative correlation between urban heat island intensity and wind speed (Kim & Baik, 2005; Morris, Simmonds, & Plummer, 2001; Oke, 1982). The effect of wind varies from region to region and could become more evident in coastal areas where heat islands interact strongly with sea-breeze circulations (Freitas, Rozoff, Cotton, & Dias, 2007). However, only a handful of studies (Bass, Krayenhoff, Martilli, & Stull, 2002; Doick, Peace, & Hutchings, 2014) considered the impact of wind pattern on the spatial distribution of temperature reduction by greenspace.

The objective of this study is to provide a first attempt to bridge this gap and quantify the scale dependence of the impact of cool and green roofs in different cities to address the following questions: Can cities mitigate heat islands with their own plans and efforts? What is a sufficient area of cool and green roofs deployment to produce a considerable cooling for urban cores? Does the scale dependence vary with geoclimatic conditions? Does the efficiency (cooling per adapted roof area) of these mitigation plans also vary with scale? To answer these questions, high-resolution simulations using the Weather Research and Forecasting model version 3.5.1 are conducted with designed scenarios of mitigation strategies at different scales.

2. Setup of numerical experiments

2.1. High-resolution weather simulations

The scale dependence of the cooling effect introduced by cool and green roofs in urban areas might be influenced by changes in geoclimatic conditions, i.e., wind, temperature, topography, humidity. In this study, we addressed this sensitivity through weather simulations over six metropolitan areas across the United States (Fig. 1a). To investigate the impact of background climate on the scale dependence, we focus on densely populated urban regions in different climatic regimes. Another selection criterion is that studied metropolitan areas have active climate action plans since the broader implications of this study are on urban heat mitigation. We selected 4 cities from the study regions included in the Urban Water Innovation Network (UWIN, https://erams.com/UWIN/): Phoenix, Miami, Los Angeles, and New York City. Chicago and Pittsburgh were then added to represent urban regions with a humid continental climate. The Köppen-Geiger climate classification of the studied metropolitan areas is summarized in Table 1.

The advanced research version 3.5.1 of the Weather Research and Forecasting (WRF) model, a non-hydrostatic weather prediction model developed by the National Center for Atmospheric Research, was used for numerical simulations in this study. The WRF model solves the fully compressible non-hydrostatic Euler equations at high-resolution over massively-parallel computing platforms. Since its release in 2000, community contributions have delivered a host of parameterization schemes for individual physical processes. More information on the WRF model can be found in a recent overview (Powers et al., 2017). The WRF model has been successfully applied over major metropolitan areas around the world, and its performance has been validated against a wide variety of observations (Chen et al., 2011). Among the available parameterization options for land surface processes, we selected the Noah land surface model for non-urban terrain and an enhanced single-layer urban canopy model for urban land surfaces following previous studies (Yang, Wang, Georgescu, Chen, & Tewari, 2016). Compared to the Noah land surface model, the urban canopy model considers the effect of canyon geometry, modified surface properties, and anthropogenic heat in solving surface energy and water budgets. The enhanced single-layer urban canopy model allows users to 1) simulate the sub-facet heterogeneity of individual urban surfaces (e.g., users can

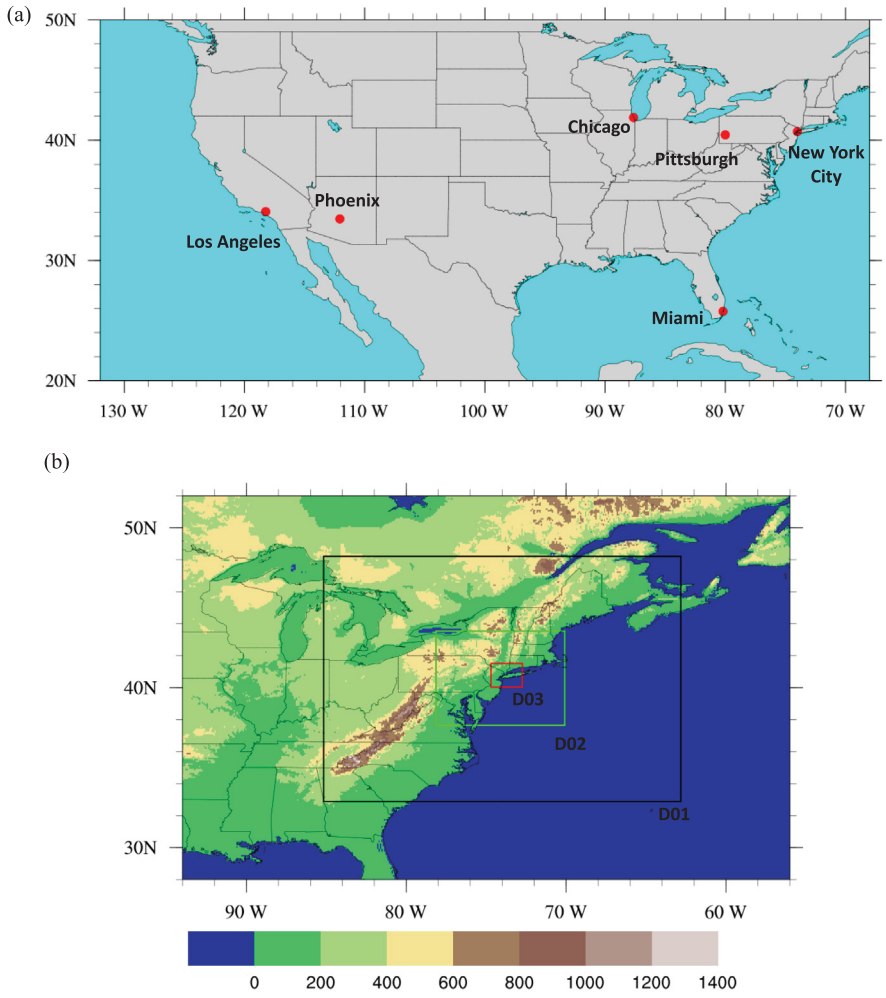

Fig. 1. Numerical experiment setup in the WRF model: (a) geographical locations of the studied metropolitan areas; (b) an example of the nested domain configuration for New York City with elevation (in meters) overlaid as a pseudocolor.

specify fractions of concrete, asphalt, and vegetated ground or roof or wall surfaces with distinct properties (Wang et al., 2013)), and 2) account for hydrological processes in the built environment (Wang et al., 2013; Yang, Wang, & Chen et al., 2015). In the WRF model, green roofs are represented by a vegetation-soil layer on top of a concrete deck. Evapotranspiration from green roofs consists of direct evaporation from soil and transpiration from leaves.

For each studied metropolitan area, we used a nested domain configuration (Fig. 1b) with grid horizontal resolutions of 9, 3, and 1 km. Simulations were driven by initial conditions from the North American Regional Reanalysis data from the National Centers for Environmental Prediction (https://rda.ucar.edu/datasets/ds608.0/). After initialization, the WRF model solves the coupled land-atmosphere system and requires input only at atmospheric boundaries. The initial and boundary conditions include meteorological variables such as wind speed, pressure, temperature, humidity, etc. (see http://www2.mmm.ucar.edu/wrf/src/fix_wps/Vtable.NARR). Land use and land cover were determined using the National Land Cover Database (NLCD) 2011 (Homer et al., 2015). Urban areas were classified into 4 land use types in the NLCD 2011, namely the high intensity, medium intensity, low intensity, and open space developed areas. A set of urban canopy parameters was assigned to each land use type, including building height, road width, and impervious fraction (see Table S1). Due to the lack of data for each individual city, we adopted the canopy parameters calibrated for Phoenix in Yang, Wang, Kaloush et al. (2016) and applied it for all studied cities. This is one limitation of the study and the benefit of accurate urban dataset is discussed in the conclusion section; however, this limitation will not affect our comparisons to deduce scale dependence since the city parameters (except intervention areas of cool and green roofs) are the same in all runs. To improve the representation of land surface heterogeneity, a mosaic approach was used to solve for multiple land use categories (Li, Bou-Zeid, Barlage, Chen, & Smith, 2013; Ramamurthy, Li, & Bou-Zeid, 2017). In each model grid cell, the land use fraction of each land cover type was estimated using the NLCD 2011, and the types with the largest eight fractions in each cell were considered in WRF simulations. The flux from each type is then weighted by its areal fraction to obtain aggregate fluxes into the atmosphere. Hydrological and thermal properties of all land cover types are prescribed in the WRF model. Compared to the default approach where fluxes are calculated only for the dominant land use type in every grid, the mosaic approach can significantly enhance the modeling of land-atmosphere exchange.

Other urban modelling options in the WRF model include a sophisticated multi-layer urban canopy model (Martilli, Clappier, & Rotach, 2002) and its improved version with a building energy model (Salamanca, Krpo, Martilli, & Clappier, 2010). They account for vertical distributions of heat and momentum in the three-dimensional urban canopy layer, and allow a direct interaction with the overlying boundary layer. However, they do not include green roof representations and do not allow for sub-facet scale heterogeneity, which precludes their use to address the questions of this study. The single-layer urban canopy model used here yields suitable predictions over 1 km

Table 1
Climate classification and scenarios of mitigation strategies at three scales for studied metropolitan areas.

Metropolitan area	Köppen-Geiger climate classification	Local scale intervention	City scale intervention	Regional scale intervention	Latest climate action or sustainability plan
Chicago	Humid continental	City center defined by the Department of Planning and Development (0.52 km^2)*	City of Chicago (14.45 km^2)	(679.19 km^2)	Chicago Climate Action Plan (City of Chicago, 2009)
Los Angeles	Mediterranean	Central Los Angeles defined by the Department of City Planning (13.13 km^2)	City of Los Angeles (101.77 km^2)	(619.09 km^2)	Community Climate Action Plan (County of Los Angeles, 2015)
Miami	Tropical monsoon	City of Miami (1.75 km^2)	Miami-Dade County municipal areas (4.30 km^2)	(221.69 km^2)	GreenPrint Plan (Miami-Dade County, 2010)
New York City	Humid subtropical	Manhattan (1.54 km^2)	New York City (30.96 km^2)	(762.50 km^2)	1.5 °C: Aligning New York City with the Paris Climate Agreement (New York City, 2017)
Phoenix	Desert	Districts 4, 7 and 8 around downtown Phoenix (11.50 km^2)	City of Phoenix (56.23 km^2)	(332.02 km^2)	2050 Environmental Sustainability goals (City of Phoenix, 2016)
Pittsburgh	Humid continental	City of Pittsburgh (4.12 km^2)	Allegheny County municipal areas (55.92 km^2)	(458.02 km^2)	Climate Action Plan 3.0 (City of Pittsburgh, 2017)

* Values in brackets denote the total area of cool roof or green roof, which are only deployed over 25% of the roofs of a city. For example, Manhattan's area is 59 km^2, so 25% of cool/green roofs (1.54 km^2) would only cover 2.5% of the total area of the borough.

grids and has been very widely validated (Chen et al., 2011; Yang, Wang, Georgescu et al., 2016). Additional motivations for adopting the single-layer urban canopy model in this study include: 1) its coupling with the mosaic approach to consider multiple land uses in every WRF grid is useful for highly heterogeneous urban terrain. This coupling has been evaluated in New York City (Ramamurthy et al., 2017) and Washington DC (Li et al., 2013), and 2) a detailed parameterization of green roofs has only been implemented in the single layer urban canopy model.

All simulations were run from 0000 UTC on 10 July to 0000 UTC on 14 August, with an output frequency of 1 h. The first 5 days (10–14 July) were treated as the spin-up period and the results were analyzed only for 15 July – 14 August. To assess the performance of mitigation strategies in a "typical" summer, we selected, for each metropolitan area, a different simulation year that has mean daily maximum and minimum air temperatures close to the 1981–2010 climate normal released by the National Centers for Environmental Information for that metropolis (NCEI, https://www.ncdc.noaa.gov/data-access/land-based-station-data/land-based-datasets/climate-normals/1981-2010-normals-data). As a result, Pittsburgh and Chicago were simulated for the year 2013, and Los Angeles, Miami, Phoenix, and New York City were simulated for the year 2014.

2.2. Scenarios of mitigation plans

In the absence of consistent federal action to mitigate climate change in the United States, many state and city governments have risen to the challenge by enacting local climate change legislation and developing a range of plans and policies (Drummond, 2010). Table 1 lists the latest climate action or sustainability plan for the metropolitan areas considered in this study. Note that Los Angeles and Miami metropolitan areas have county-level plans, while Phoenix, New York City, Pittsburgh, and Chicago have city-level plans. The primary goal of these plans is to reduce greenhouse gas emissions, but the need for mitigating the urban heat island effects is explicitly outlined since heat islands increase the cooling energy consumption and exacerbate extreme heat. The use of green roofs is recognized by Chicago and New York City because of the insulation effect during both hot and cold months (City of Chicago, 2009; New York City, 2017). In Pittsburgh's climate action plan, green roofs are promoted considering their co-benefit in sustaining local food security (City of Pittsburgh, 2017). On the other hand, Los Angeles County recommends the adoption of cool roofs due to their competitive prices and ease of installation (County of Los Angeles, 2015). To obtain conceivable scenarios of mitigation plans, we examined the land use planning and development map for each studied metropolitan area and identified three (local, city, and regional) plausible levels of implementation (Table 1). Green and cool roofs are installed over built terrains defined by the National Land Cover Database 2011, and colored areas in Fig. 2 illustrate the spatial extent of these built surfaces at the various implementation levels. It is worth mentioning that to attain a sufficient footprint of cool roof or green roof area, mitigation plans at the city level may not correspond to the political or administrative boundaries of the studied cities. For the largest regional intervention, for example, the whole metropolitan area of each city is targeted.

To quantify the consequence of mitigation plans at different scales, we used the NLCD 2011 with conventional concrete roofs (hereinafter control scenarios) to represent the current landscape of individual metropolitan areas; its albedo is 0.3. For cool roof and green roof scenarios, we assumed a 25% areal coverage on building rooftops. This fraction is at the lower end of previous numerical studies (Li et al., 2014; Yang, Wang, & Chen et al., 2015), but is still in fact beyond the practical implementation potential in the foreseeable future. A set of four simulations was carried out for each metropolitan area in this study to estimate the cooling benefit from local (~1–10 km^2), city (~10–100 km^2), and regional (~500 km^2) deployment of adapted

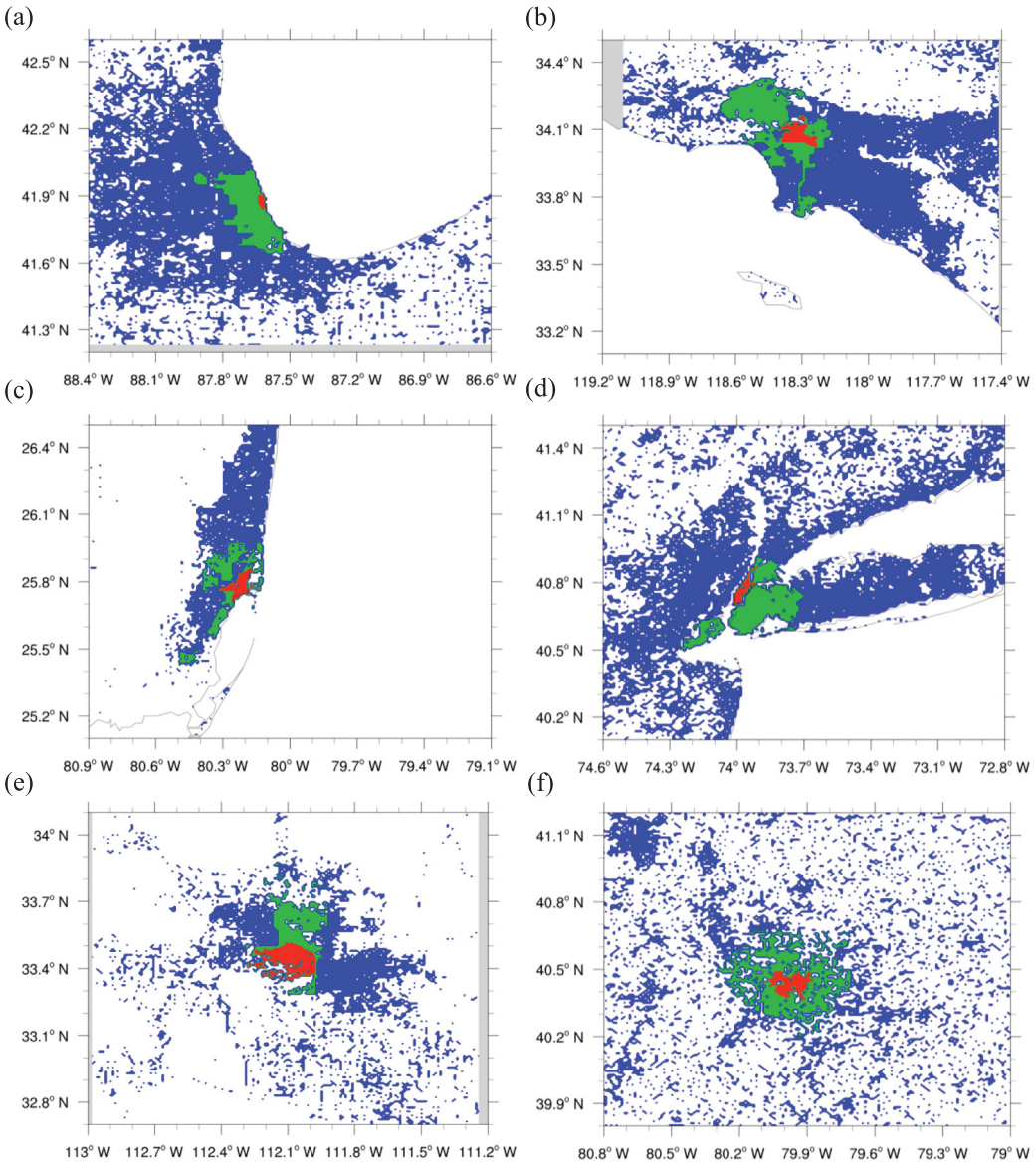

Fig. 2. Spatial extent of mitigation plans at local (red), city (green), and regional (blue) scales in (a) Chicago, (b) Los Angeles, (c) Miami, (d) New York City, (e) Phoenix, and (f) Pittsburgh. (For interpretation of the references to colour in this figure legend, the reader is referred to the web version of this article.)

roofs, relative to the control baseline with no intervention. The selection of physical boundaries of the local and city scale interventions is explained in Table 1. Simulated scenarios of mitigation strategies at the regional scale are comparable to those assuming a uniform deployment in previous studies, except that the areal coverage is 25% of the roof area (for Manhattan that is only about 2.5% of the total area of the borough for the local-scale implementation). Total areas converted to cool or green roofs in all scenarios are listed in Table 1. To focus on the effect of geoclimatic conditions, green roofs were assumed to be well irrigated with an evapotranspiration efficiency of 75% (of their potential evaporation rate) in all runs to exclude the impact of water availability. In addition, the albedo of green roofs was set equal to baseline conventional roofs to isolate the effect of evaporative cooling. Following previous studies (Li et al., 2014; Wang et al., 2013), the properties of different roofs were set to (1) conventional roof: albedo (r) = 0.3, thermal conductivity (k) = 1.0 W m^{-1} K^{-1}, heat capacity (C) = 2.0 MJ m^{-3} K^{-1}; (2) green roof: r = 0.3, k = 1.1 W m^{-1} K^{-1}, C = 1.9 MJ m^{-3} K^{-1}, leaf area index = 5; and (3) cool roof: r = 0.7, k = 1.0 W m^{-1} K^{-1}, C = 2.0 MJ m^{-3} K^{-1}. Due to model limitations, the modification of roughness length over green roofs is not considered. Individual roofs were assumed to be vertically homogeneous in all simulations such that their thermal properties do not vary with depth. One here should note that both the 75% evaporation rate of green roofs and the 0.7 albedo of cool roofs are on the high end and would require roof maintenance and irrigation to be sustained.

3. Model evaluation

The WRF simulations of control scenarios for the studied metropolitan areas are evaluated against ground-based meteorological observations. Aiming to quantify the scale dependence of cooling effects by cool and green roofs, in this paper we focus on the model's ability in predicting 2-m air temperature (T_2). Hourly measurements of T_2 were collected from the National Centers for Environmental Information (https://data.noaa.gov/dataset/integrated-surface-global-hourly-data). One airport station and two non-airport stations are used for each metropolitan area (detailed in Table S2). Due to data availability, two airport stations are used for Pittsburgh. The comparison of 2-m air temperature between these ground observations and the model prediction at the nearest grid cell is shown in Fig. S1. During the

study period, air temperatures have a wide range among the six cities, from the night-time lows of about 10 °C in Pittsburgh to the daytime highs of about 42 °C in Phoenix. Significant intra-city variations are also observed, especially in Los Angeles, where the downtown station measures much higher temperatures than the other two stations. The WRF model is able to capture the temperature variation reasonably well over all stations in all metropolitan areas. Root-mean-square errors (RMSEs) of predicted T_2 range from 0.87 °C in Chicago Northerly Island to 1.84 °C in Phoenix Sky Harbor airport (reported in Table S2). Average RMSE over all stations is the largest in Miami, where the largest absolute error was about 7 °C and occurred after the WRF model failed to capture an intense precipitation event. Overall, model performance in this study is comparable to previous high-resolution WRF urban simulations (Ramamurthy et al., 2017; Sharma et al., 2016). One can thus conclude that the urban climate in the studied cities is reproduced by the WRF simulations with adequate accuracy and can be used with confidence to explore the cooling effect of cool and green roofs.

The implementation of green and cool roofs in WRF cannot be directly validated, because the model grid size (1 km in this study) is much larger than building rooftops where field experiments have been conducted. Nevertheless, the same urban canopy model implemented here in WRF has been validated in "offline mode" (interactions between urban land and overlying atmosphere are turned off) under the forcing of atmospheric observations (Ramamurthy et al., 2015; Sun, Bou-Zeid, Wang, Zerba, & Ni, 2013). The offline UCM can be applied over the canyon scale (~10–100 m), and therefore its simulated effects of green and cool roofs can be evaluated against in-situ measurements. More specifically, compared with observations over cool roofs, Ramamurthy et al. (2015) showed the urban canopy model can capture roof surface temperatures and heat fluxes with RMSEs of 7.30 °C and 7.88 W m^{-2}, respectively. Sun et al. (2013) evaluated the model's performance in simulating surface temperatures and volumetric water content in the medium layer of green roofs. Though quantitative errors were not reported, a good agreement was found between model predictions and experimental measurements at two sites in Beijing, China and in Princeton, USA.

4. Results and discussions

4.1. Scale dependence of cooling benefits

Areas covered by the local-scale plans are the urban cores of the studied metropolitan areas and serve as the centers of commercial, cultural, and political activities. These central areas normally have the highest temperature and population density within the city, and consequently it is important to know how mitigation plans at different scales will affect them. For this purpose, we first focus on the reduction in T_2 over the local-scale planning area (red areas in Fig. 2) and neglect the cooling outside even for scenarios with regional-scale interventions. Fig. 3 compares the diurnal profiles, averaged over all simulated days, of urban core cooling achieved by implementing green roofs at the three scales. With local scale interventions, all urban cores receive very limited cooling of less than 0.1 °C throughout the diurnal cycle. When green roofs are deployed at the regional scale, only urban cores in New York City, Los Angeles and Pittsburgh receive a significantly larger cooling compared to the local scale. Temperature reductions in New York City and Los Angeles also show a significant hourly variation. While differences in the absolute magnitude of cooling in the various cities can be noted, the most striking difference among the cities is how their T_2 reductions change with the scale of green roof deployment.

In New York City, Los Angeles and Pittsburgh, the cooling of urban cores increases considerably with expansion of the area of green roofs (Fig. 3b, d and f). When implementation of green roofs is upscaled from the local to the regional level, reduction of daytime mean T_2 increases from 0.03 °C to 0.21 °C for New York City, from 0.03 °C to 0.12 °C for Pittsburgh, and from 0.05 °C to 0.18 °C for Los Angeles. Temperature reductions in Chicago, Miami and Phoenix, on the other hand, show minor sensitivity to the mitigation plans (Fig. 3a, c and e). Taking Chicago as an example, daytime mean T_2 over the city centre is reduced only by an additional 0.02 °C upon increasing green roof areas from 0.52 km^2 in the local plan to 679.19 km^2 in the regional plan. During night-time, temperature reductions by green roofs are much smaller because incoming shortwave radiation is unavailable to drive evapotranspiration (but some benefits still exist due to reduced heat storage during the day and due to limited evaporation). The scale dependence of night-time cooling for individual metropolitan areas is nevertheless consistent with the daytime trend, and the benefit of green roofs continues to scale better in New York City, Los Angeles and Pittsburgh.

To better understand the difference in cooling among the studied cities, we further look into the temporal variation of urban core cooling by green roofs at local, city, and regional scales. Daily maximum cooling in T_2 (the largest temperature reduction by green roofs within a 24-hours period) for every day in the simulation period is plotted in Fig. 4. Though local scale interventions lead to very limited cooling in monthly mean diurnal profiles (Fig. 3), Fig. 4 shows that they are able to more significantly reduce the maximum urban core temperatures on some days. Among the studied cities, the largest daily maximum cooling of 0.86 °C by the local plan is found in Chicago, while the smallest daily maximum cooling of 0.31 °C occurs at Pittsburgh. With regional plans of green roof deployment, the largest daily maximum cooling over urban cores can be up to about 1.5 °C in Chicago and New York City. Note that daily maximum cooling scales with green roof intervention areas in New York City, Los Angeles and Pittsburgh on most days. In Chicago, Miami and Phoenix, however, the scaling of daily maximum cooling is only found during a few days where large temperature reductions are found. The gap between monthly mean cooling and maximum cooling is explored and explained in Section 4.2.

The magnitude of the monthly mean temperature reduction from regional plans that we find in this study is consistent with the previous numerical study of Li et al. (2014) for Baltimore, MD, that examined how the cooling benefits increase with the fraction of upgraded roofs (from 10 to 100%), but only simulated interventions over the whole metropolitan area. It is noteworthy that some previous studies observed daytime air warming and night-time air cooling over green roofs (Solcerova, van de Ven, Wang, Rijsdijk, & van de Giesen, 2017; Speak, Rothwell, Lindley, & Smith, 2013). The cooling impact of green roofs can vary significantly with the cover plant species. Over Sedum-covered green roofs, the stomata of plants close to prevent water loss in the afternoon and open at night (since Sedum operates as a CAM plant under water stress). As a result, evapotranspiration is more active at night than in the day and creates evident nocturnal cooling. These "desert" plants are not the most effective for cooling on green roofs. In this study, we simulated herbaceous green roofs with a large leaf area index of 5 under well-irrigated conditions. Evapotranspiration over green roofs is active throughout the day, and reaches its maximum around noon time with the strongest incoming solar radiation. This explains the simulated larger daytime cooling effect of green roofs in our study.

4.2. Spatial variation of cooling benefits

To understand the disparities in the scale dependence of the cooling benefits of green roofs amongst cities, in this section, we look into the spatial distribution of monthly mean T_2 reductions. Results at 1600 local time are depicted as regional maps of T_2 reductions during daytime (Fig. 5), showing the T_2 reductions in New York City and Chicago with 10-m wind vectors for the fine-resolution domain. Fig. 5a demonstrates that installing green roofs at the local scale leads to a minor cooling over Manhattan (outlined in red), which is smaller than the cooling obtained by a local-scale intervention in Chicago (Fig. 3a and d). The cooling benefit of greening 25% of Manhattan's rooftops seems

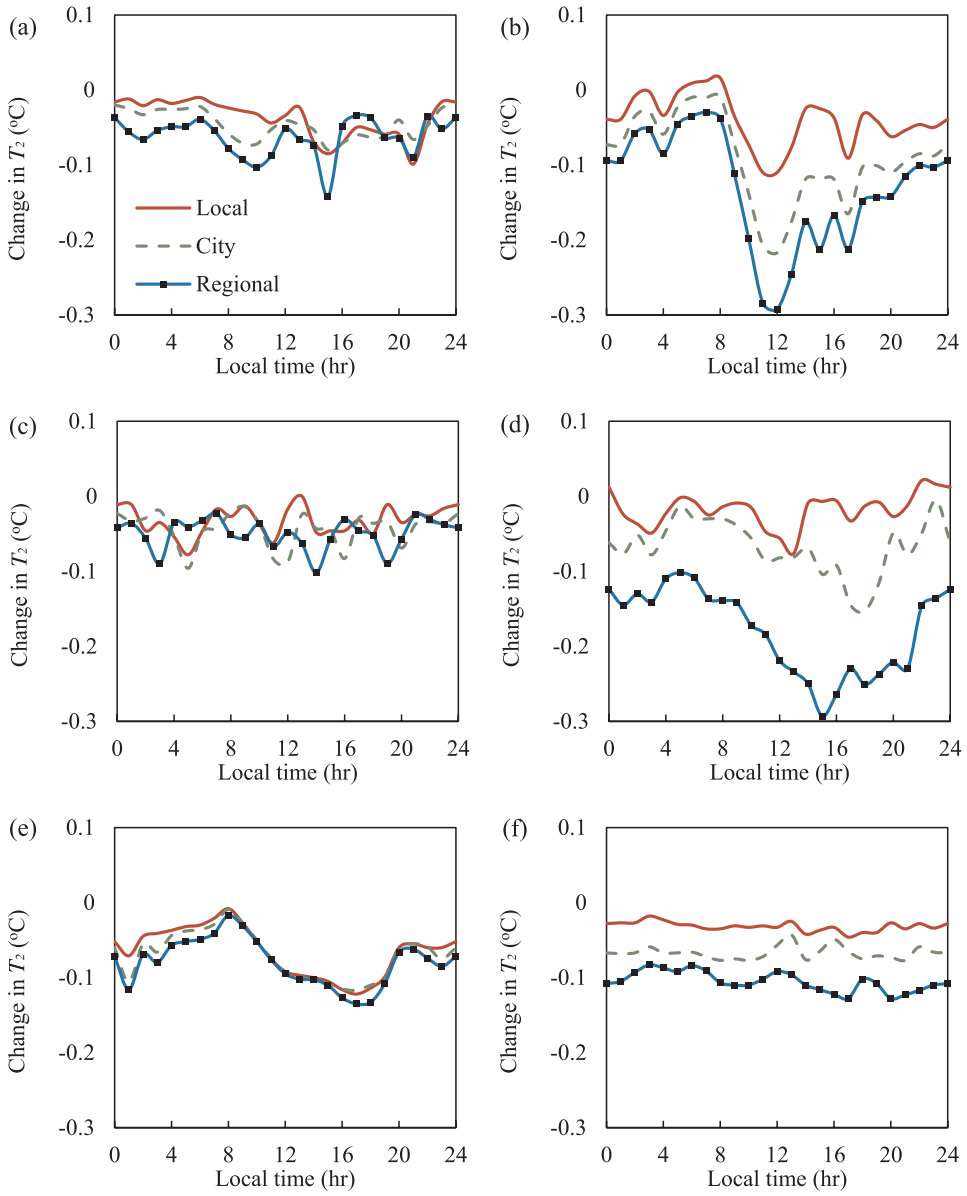

Fig. 3. Averaged diurnal profiles of the change in T_2, by green roofs at local, city, and regional scales over the urban cores of (a) Chicago, (b) Los Angeles, (c) Miami, (d) New York City, (e) Phoenix, and (f) Pittsburgh. (For interpretation of the references to colour in this figure legend, the reader is referred to the web version of this article.)

to be transported by the sea breeze towards inland areas, where a small cooling is observed to the north of New York City (though the small magnitude puts the robustness of this inland cooling into question). When green roofs are adopted at the city scale, Manhattan is able to achieve a reduction of about 0.15 °C in mean T_2 at 1600 local time (Fig. 5c). This is due to the surface cooling in upwind urban areas to the south of Manhattan (see green boundaries in Fig. 5c) that is now influencing air temperature in Manhattan. With a uniform implementation of green roofs over the entire metropolitan area, the regional plan can reduce monthly mean T_2 over Manhattan by about 0.26 °C at 1600 local time (Fig. 5e). Compared to the local mitigation plan, the city and regional plans provide additional cooling benefits for Manhattan by greening its upwind areas. Due to the penetration of sea breeze during that period, green roof plans at the city and regional levels also create important cooling benefits for downwind inland areas (New Jersey and New York state). The maximum cooling at 1600 local time is consistently found to the north (exactly downwind) of New York City. Similarly, the strong scale dependence of the cooling benefits in Los Angeles and Pittsburgh are caused by implementing green roofs over buildings in upwind areas, relative to the urban core, in city and regional plans (see wind patterns in Fig. S2). This significant scale dependence in NYC, LA, and Pittsburgh indicates that the wind pattern and shape of metropolitan area regulate the daytime cooling from green roofs in these cities. For reducing daytime temperatures in urban cores, the southern part in New York City, the south-western part in Los Angeles and the western part in Pittsburgh are better locations for intervention, but only if the wind patterns that these cities experience for the simulated months remain dominant.

With smaller wind speeds for the simulated period, the cooling effect of green roofs is more localized in Chicago than in New York City. At 1600 local time, the average 10-m wind speed is 4.14 m s^{-1} over New York City and 2.73 m s^{-1} over Chicago. At all three intervention levels, urban areas with green roofs in Chicago are able to receive a noticeable temperature reduction (Fig. 5b, d and f) (higher than that of Manhattan for the local-scale intervention). However, upscaling the mitigation plan for Chicago involves mainly altering downwind built

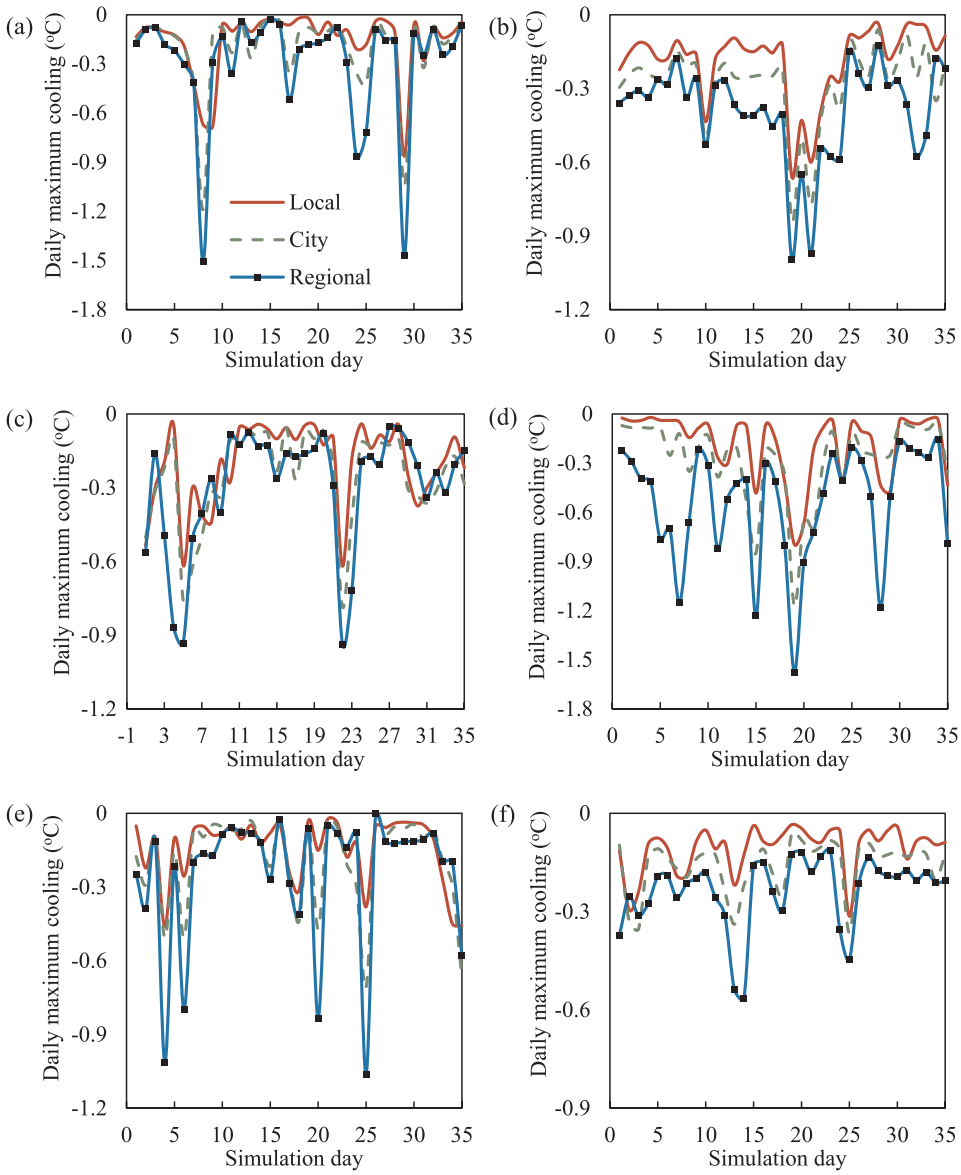

Fig. 4. Daily maximum cooling in T_2 over the urban cores by green roofs at local, city, and regional scales during the simulation period in (a) Chicago, (b) Los Angeles, (c) Miami, (d) New York City, (e) Phoenix, and (f) Pittsburgh. (For interpretation of the references to colour in this figure legend, the reader is referred to the web version of this article.)

areas; consequently, the cooling benefits from the additional green roofs are not transported towards the city center and a weak scale dependence is found (Fig. 3a). Reductions in monthly mean T_2 from green roofs is hence more homogeneous and the cooling is significantly smaller in Chicago than in New York City. Similarly, the Miami metropolitan area has an elongated shape along the coastline, and since winds mainly blow perpendicular to the coast, most cooling benefits from green roofs at city and regional scales are carried inland by the southeast wind (Fig. S3). In Phoenix, west wind dominates at 1600 local time that additional green roofs over the eastern part of metropolitan area in the regional plan are not effective in cooling the urban core (Fig. S3). The weak scale dependence again illustrates the importance of intervention location within the metropolitan areas.

Maps of monthly mean T_2 reductions at 0100 local time are shown in Fig. 6 for NYC, LA, and Pittsburgh for the city and regional interventions only. While evapotranspiration is reduced during night-time, all the green areas will have a lower heat storage and temperature due to the thermal energy they dissipated during the daytime by evaporation. Compared to daytime results, wind speed is notably smaller at night and the wind pattern changes significantly. In New York City, the cooling effect from regional deployment of green roofs is relatively homogenous under the weak land breeze at 0100 local time (Fig. 6b). Large reductions in T_2 to the north of New York City at 1600 local time disappear at night. With the city scale intervention, only a small fraction of New York City receives cooling greater than 0.1 °C. This is caused by the smaller cooling capacity of green roofs during night-time. As evapotranspirative cooling is less active at night, a larger spatial coverage of green roofs is required to create a noticeable reduction of T_2. Similarly in Los Angeles (Fig. 6c and d) and Pittsburgh (Fig. 6e and f), spatial distributions of T_2 reductions at 0100 local time are significantly different from those at 1600 local time due to the change in wind patterns. Night-time temperature reductions with local scale mitigation plans are very small in all metropolitan areas and hence the results are not plotted here. This implies that under night-time low wind conditions, the spatial coverage of green roofs becomes important and the intervention location within the metropolitan area has a lesser impact. In Chicago, Phoenix and Miami, reductions in monthly mean T2 by green roofs during night-time are relatively smaller than for the

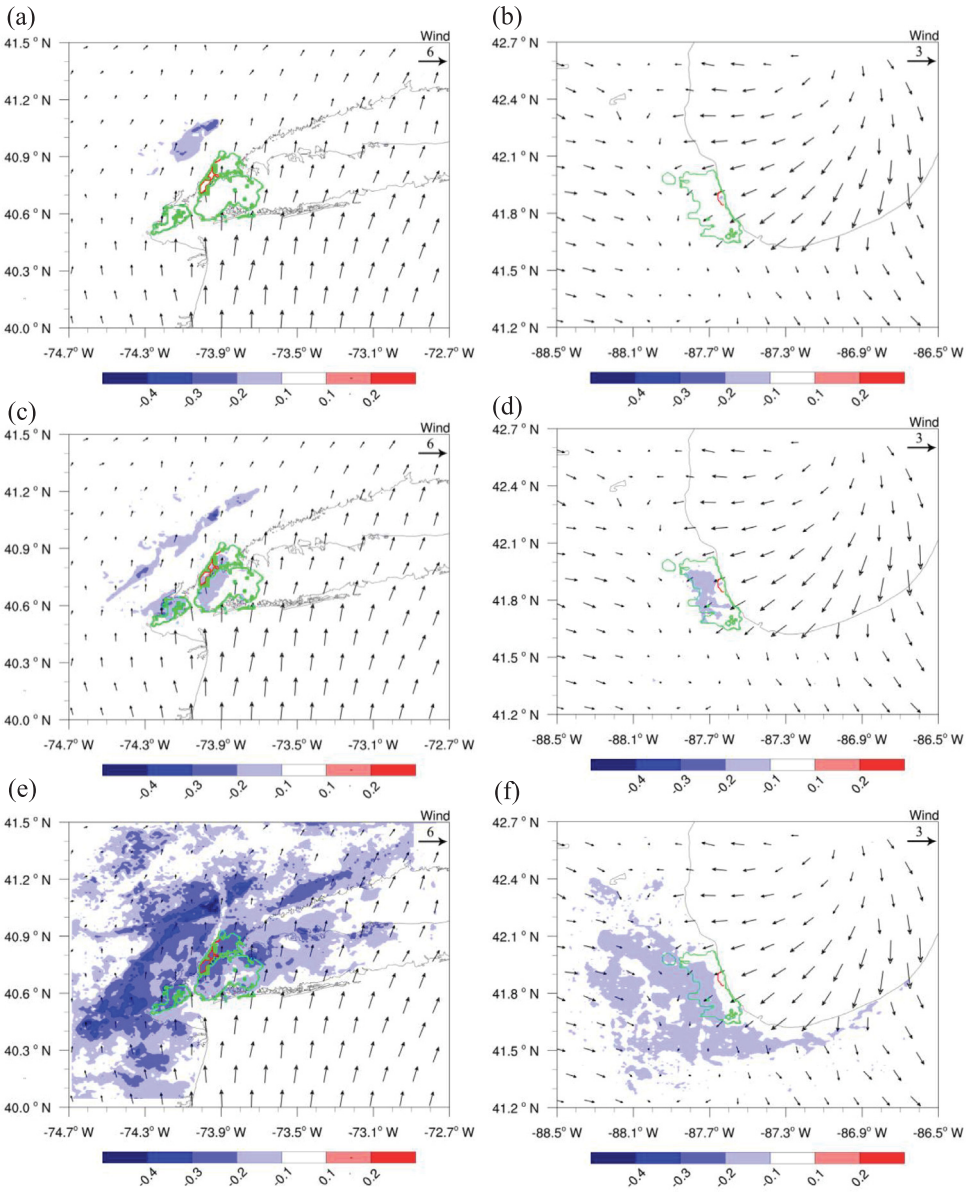

Fig. 5. Simulated monthly mean T_2 reductions at 1600 local time with 10-m wind vectors overlaid from green roof deployment at the (a) local, (c) city, (e) regional scales in New York City and (b) local, (d) city, (e) regional scales in Chicago. (For interpretation of the references to colour in this figure legend, the reader is referred to the web version of this article.)

other cities (Fig. S4).

Fig. 4 illustrates that the maximum temperature reduction by green roofs can be multiple times greater than the monthly mean reduction. To understand what causes the higher cooling benefit of green roofs during individual days, we analyse the spatial distribution of T_2 reductions at the time corresponding to the largest daily maximum cooling for a given city in Fig. 4. Results of local and regional scale interventions are shown in Figs. 7 and S5, respectively. Minor warming signals by green roofs are found in some regions in the snapshot (probably due to changes in wind patterns by the roofs), but they cancel out when averaged at the monthly scale. Instantaneous regional wind patterns in Fig. 7 are significantly different from the averaged ones in Fig. 5. In Chicago, New York City and Miami, wind converges over the urban core making the cooling benefit of local scale interventions very evident. Maximum reductions in T_2 in Fig. 7 from local interventions are found to be larger than the averaged reduction from regional plans in Figs. 5, S2 and S3. The large cooling benefits also emerge at the convergence zone of wind when green roofs are installed at the regional scale (see Fig. S5). In Pittsburgh, wind does not converge on the urban core under the strong southward advection. As a result, the maximum cooling by the local plan is much smaller than those in other cities. In LA and Phoenix, the maximum cooling is caused by slow winds around the urban core (Fig. 7b and e), which allow cooling effects by green roofs to stay local. Consequently, downwind cooling effects in the monthly mean results (e.g., Figs. S2 and S3) are not observed, the cooling is rather strongly variable but remains tightly linked to wind patterns. It is noteworthy that the maximum cooling by green roofs in all studied cities is observed between 1300 and 2000 local time, but it does not occur on the hottest day during the simulation period. This again supports the finding that the wind pattern and shape of metropolitan area play a crucial role in determining the cooling impact of green roofs, and as a result the cooling might not be delivered when most needed, i.e. during the hottest days.

To summarize, the comparison between the results in the six cities demonstrates that both the shape and setting of the metropolitan area, particularly the location of the urban core relative to the wider

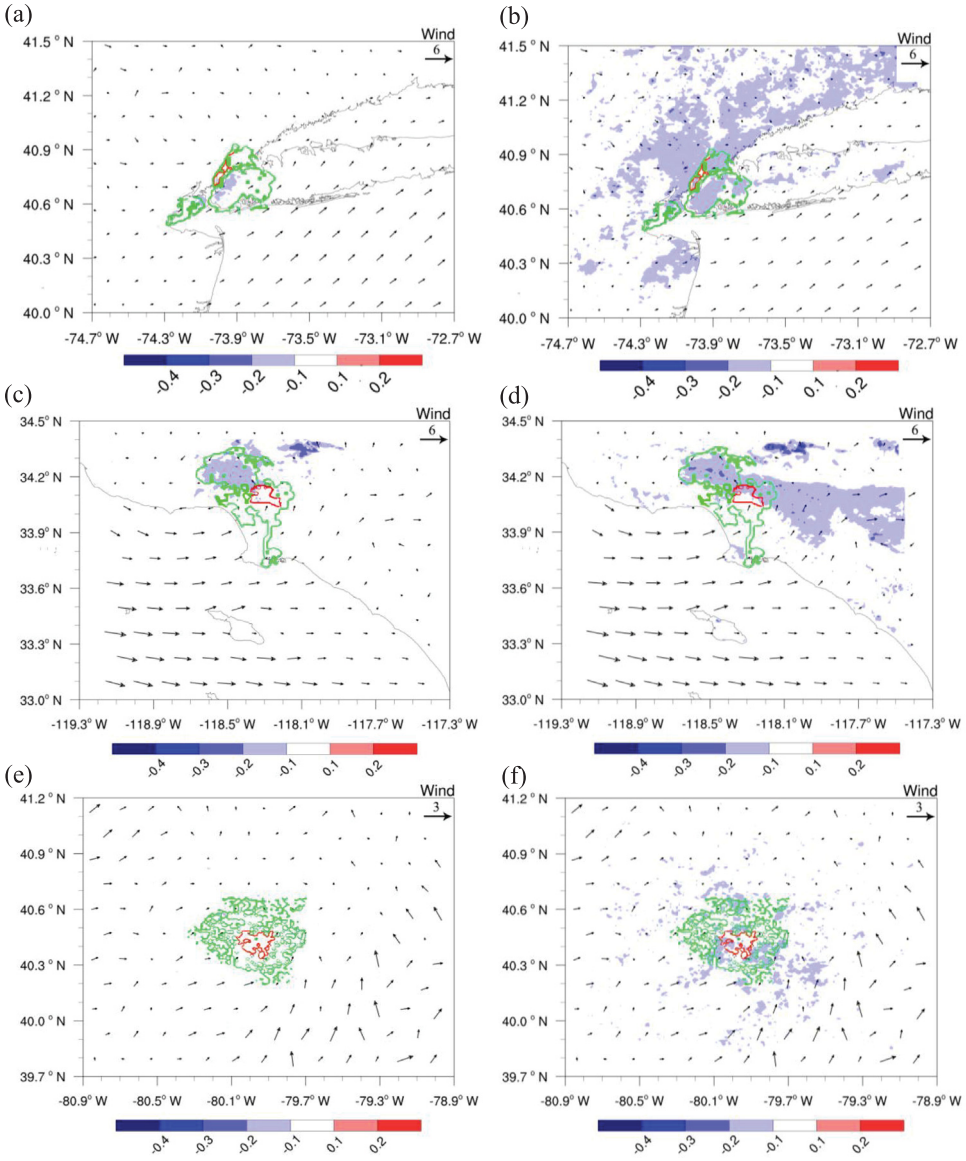

Fig. 6. Simulated monthly mean T_2 reductions at 0100 local time with 10-m wind vectors overlaid from green roof deployment at the city scale in (a) New York City, (c) Los Angeles, (e) Pittsburgh and the region scale in (b) New York City, (d) Los Angeles, (f) Pittsburgh. (For interpretation of the references to colour in this figure legend, the reader is referred to the web version of this article.)

metropolis, and the geoclimatic conditions, particular wind patterns, play important roles in regulating the regional benefits of green roofs. We point out that the modification of roughness length by vegetation over green roofs is not considered in this study as it is not expected to have a significant impact on the wind speeds (dominated by building-scale roughness) or on the sensible/latent heat partitioning (since the roughness lengths for sensible and latent hat fluxes must be maintained equal). Greening 25% of building rooftops therefore, even over the entire metropolitan area, has a negligible impact on the regional 10-m wind patterns.

To examine whether the scale dependence is unique to green roofs, we simulated the same planning scenarios with cool roofs for Chicago and New York City. The scale dependence of cooling benefits by cool roofs is comparable to that of green roofs. The spatial distribution of T_2 reduction by cool roofs at 1600 local time is shown in Fig. S6. Reductions in T_2 by cool roofs show a weak relationship with the scale of the mitigation plan in Chicago, but are sensitive to the implementation area in New York City. For both cities, cool roofs provide a stronger daytime cooling for urban cores than green roofs when deployed at local and city scales (though one should be cautious in generalizing this statement since it depends on the imposed albedo of the cool roofs and the evaporative efficiency of the green roofs). Compared to Fig. 5, the similar cooling pattern suggests that geoclimatic conditions control the regional effect of the studied mitigation strategies more than roof properties.

Increasing the spatial extent of mitigation strategies is commonly treated as an effective way to mitigate heat islands. The broader the intervention area, the larger the temperature reduction. This hypothesis is overall reasonable in terms of long-term regional average temperature for individual metropolitan areas. When targeting urban cores, however, the scale dependence reported in this section reveals that the location of the mitigation measures is important, especially under windy conditions. Regional wind patterns play a more important role than other climatic variables (e.g., climatic mean of temperature and humidity) in controlling the benefit of green roofs, such that the scale dependence of green roof cooling is not related to the Köppen-Geiger climate classification. Extensive mitigation initiatives and efforts in areas downwind from the core cannot in general provide significant

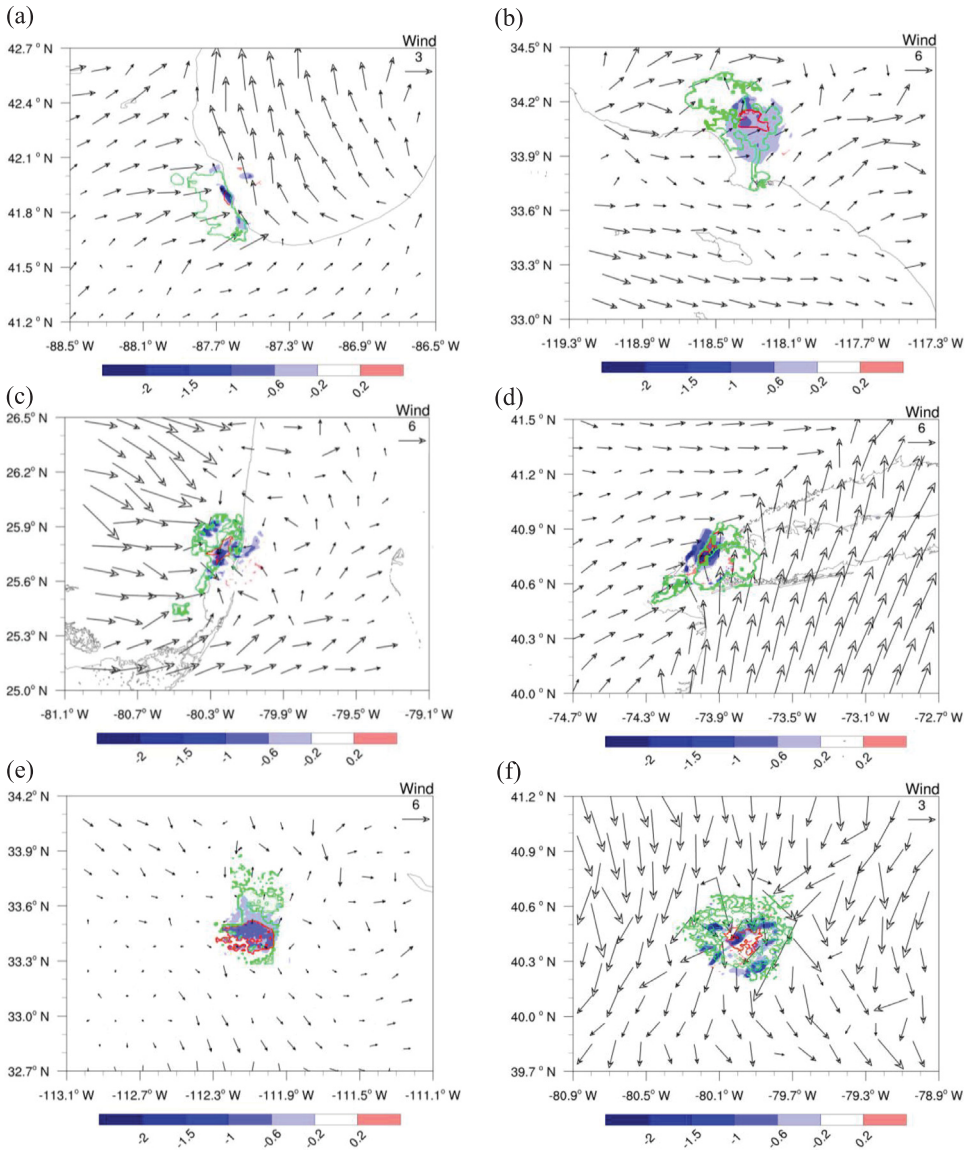

Fig. 7. Simulated maximum T_2 reductions over the urban core during the simulation period with 10-m wind vectors overlaid from green roof deployment at the local scale in (a) Chicago, (b) Los Angeles, (c) Miami, (d) New York City, (e) Phoenix, and (f) Pittsburgh. (For interpretation of the references to colour in this figure legend, the reader is referred to the web version of this article.)

additional benefits (though wind patterns are variable as we illustrated). This finding has important implications for city planners: heat mitigation strategies should focus on areas generally upwind of the urban core, although this is not always possible since for example in Chicago this upwind area might be covered by a lake when the winds are easterly. At night-time with low wind speeds, the spatial coverage of green and cool roofs becomes important and the effects remain more localized. Previous studies have investigated the effect of urban morphology on heat island and its mitigation (Steeneveld, Koopmans, Heusinkveld, Van Hove, & Holtslag, 2011; Yuan & Chen, 2011), but they focused on canyon and building geometry at the neighborhood scale. Our results here demonstrate that the shape of metropolitan area as a whole needs to be considered in designing mitigation plans. It is also worth pointing out that the cooling benefits of green and cool roofs reported here correspond to a typical summer close to the mean of 1981–2010 climate. Global climate change and continuous urbanization are projected to cause substantial temperature rise and more extreme heat events in the future (McCarthy, Best, & Betts, 2010). Cooling benefits provided by the mitigation strategies under such circumstances will become vital for cities and should be the focus of future studies.

4.3. Scale dependence of cooling efficiency

While the overall trend of the scale dependence of cooling benefits is expected – urban areas will receive a larger temperature reduction as they implement mitigation strategies at a larger scale – our results so far have shown that the magnitude of these benefits can vary significantly. It is thus not possible to propose generalizable scaling relations for urban core absolute cooling as a function of the spatial extent of the mitigation intervention. In addition, upscaling mitigation plans is associated with increased economic costs even over cities where such upscaling results in significant cooling. City-scale or regional policies to implement such strategies must therefore be economically efficient if they are to be acceptable to stakeholders and decision-makers. To evaluate the cost-benefit balance of heat island mitigation plans for the various cities, we must first estimate the cooling efficiency per unit area of cool or green roofs at different scales in the studied metropolitan areas. Because cool and green roofs can generate cooling benefits for downwind areas, here we will consider the reductions of 2-m air temperature over the entire fine-resolution domain rather than focusing on the urban cores. The cooling efficiency CE is computed as:

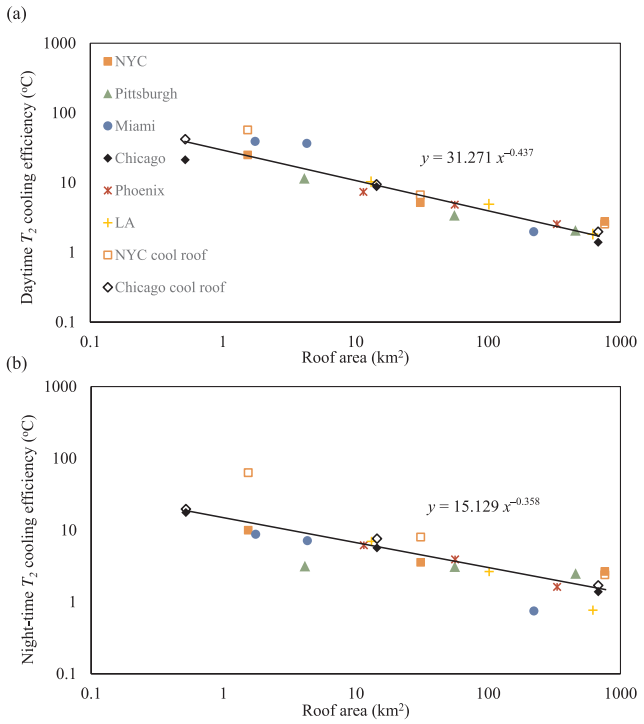

Fig. 8. Scale dependence of the cooling efficiency of mitigation strategies during (a) daytime (0700-2000 local time), and (b) night-time (2100-0600 local time).

$$\mathrm{CE}\,(z) = \frac{\sum_{x=1}^{N_x}\sum_{y=1}^{N_y}\Delta T_{x,y}(z)A_{\mathrm{grid}}}{A_{\mathrm{int}}}, \quad (1)$$

where N_x and N_y are the total number of grid cells in the x and y directions; $\Delta T_{x,y}(z)$ is the temperature drop at height z in each grid cell in the fine-resolution domain relative to the baseline; A_{grid} and A_{int} denote the area of a model grid cell and of the intervention footprint, respectively. In this study we focus on 2-m air temperature and use the corresponding T_2 for $\Delta T_{x,y}(z)$. The numerator has units of °C m^2 and is the total cooling over the whole 2-m air layer considered; the full equation has units of °C m^2 per m^2 of green/cool roofs deployed, i.e. °C. The way to interpret the numerical value of CE is as follows: a cooling efficiency of 10 °C, for example, implies that deploying a cool or green surface over 1 m^2 would result in a 10 °C cooling if constrained to influence T_2 only over that 1 m^2, or more realistically it would result in a 1 °C over an area of 10 m^2 or a 0.1 °C over an area of 100 m^2. This also explains why, unlike the results for total urban core cooling, the cooling efficiency scaling is reasonably consistent for all six cities, as depicted in Fig. 8. CE is less dependent on wind conditions and urban shape since it represents the domain-integrated total reduction in ΔT_2 and in surface-to-air heat flow resulting from one unit area of green or cool roof deployment. When the whole regional domain is taken into consideration, the cooling benefits of cool and green roofs transported downwind remain in the metropolitan regions and contribute towards the computed cooling efficiency.

The simulations also indicate that the cooling efficiency decreases rapidly with the implementation scale (Fig. 8). On a log-log graph, the linear decrease of cooling efficiency with the roof area across all studied metropolitan areas indicates an underlying power law relation between the two. When deployed with an area of about 1.6 km^2 (e.g., local plans in New York City and Miami), daytime and night-time T_2 cooling efficiencies are about 30 °C and 10 °C, respectively. At the regional scale, the maximum efficiency is found at New York City, which is about 2 °C. This decline in cooling efficiency with intervention scale is physically related to the larger decrease in air temperature (relative to baseline) with expanding intervention, leading to a smaller decrease in surface heat flux (again relative to baseline).

Cool roofs have a higher cooling efficiency than green roofs in reducing regional T_2, but again this relative difference is related to the imposed albedo of the cool roofs and the evaporative efficiency of the green roofs. Under scenarios of local-scale deployment, daytime efficiency of cool roofs is about 52 °C in New York City and 42 °C in Chicago, which is about twice the efficiency of green roofs. The difference in cooling efficiency between green and cool roofs diminishes as the intervention area increases and becomes 0.3 °C in New York City and 0.6 °C in Chicago at the region scale. Nevertheless, the scale dependence of the efficiencies of cool and green roofs is similar.

5. Conclusions

This paper examines the scale dependence of cooling benefits and efficiency of cool and green roofs for mitigating summertime urban heat islands. Six major U.S. metropolitan areas, with active climate action plans in different geoclimatic zones, are selected for the comparative study. We find that the scale dependence of reduction in 2-m air temperature over urban cores is controlled by the shape and setting of metropolitan area, particularly the location of the urban core relative to the wider metropolis, and its geoclimatic conditions, particular wind patterns. When city centers retrofit 25% of their own rooftops, though they can receive cooling up to 0.86 °C under certain favorable conditions, the monthly mean daytime temperature reduction is very limited (< 0.3 °C for the largest scale deployment). Interventions should focus on areas upwind of the urban core to maximize the regional cooling benefits in that core. Although wind direction varies continuously, planners might be able to identify the most probable wind directions for individual metropolitan regions, especially during extreme heat events. During windy periods, these upwind areas are critical to the climate in the city. On the other hand, during periods of calm weather, the benefits of cool and green roofs are more localized such that their spatial coverage becomes important.

In contrast to the absolute cooling of the urban core, the cooling efficiency, defined as the integrated reduction in 2 m air temperature over the whole domain per unit of cool or green roof deployment, showed remarkably universal scaling across all six metropoles. This cooling efficiency however decreased rapidly with increasing implementation scale. Thus, while deploying green and cool roofs at the regional scale provides additional reductions in near-surface air temperature, the daytime cooling efficiency of 2 °C is about 6% of that in the local scale mitigation plan. The CE decline has implications for deployment of green and cool roof: city planners need to balance their goal of temperature reduction with the intervention scale to sustain efficient urban heat mitigation.

With scenarios derived from cities' land use development map, this study provides new insight into effective planning and management of heat island mitigation. Though the findings from are obtained with scenarios of 25% areal coverage, previous studies indicate that, given a fixed spatial area over which green and cool roofs are to be deployed (local to regional), the resulting temperature reductions scale linearly with their fractions on buildings (Li et al., 2014). For example, the cooling from 100% deployment would be roughly about 4 times the one we report here (which is based on 25% deployment) for any scale of intervention. Hence the scale dependence reported in this study is independent from the influence of the fraction of green and cool roofs, though the absolute temperature reduction changes with the fraction. Cool and green roofs also have a direct impact on the energy consumption of the buildings on which they are installed. In terms of cooling the urban environment however, the effect is more indirect and cities should account for this scale dependence and for their unique geoclimatic setting and the location of their urban cores related to the wider metropolis. Cities also might need to work with surrounding areas to ensure the temperature reductions achieved match their

expectations and to avoid inefficient mitigation strategies in their development plans.

Despite the use of enhanced urban model, one remaining limitation of this study is the simplified characterization of heterogeneous urban landscape. In our WRF simulations, urban areas are classified only into 4 groups based on NLCD 2011 data and urban canopy parameters are identical within each group. This classification does not consider the strong spatial variation of the thermal properties of urban landscape such as surface admittance and albedo, and of physical properties such as roughness length and sky view factor. To overcome these barriers, the World Urban Database and Access Portal Tool project (WUDAPT, http://www.wudapt.org/) has been initiated to create a coherent global dataset of urban canopy parameters for urban climate research (Ching et al., 2018). Built upon the local climate zone (LCZ) classification system, a universal climate-based classification for global cities (Stewart & Oke, 2012), WUDAPT protocol can provide urban fabric characteristics specific to each neighbourhood and grid cell, and better inform parameter selections for model applications over specific metropolitan areas. A pioneering study used the dataset for Madrid, Spain and found improved performances of the WRF model (Brousse, Martilli, Foley, Mills, & Bechtel, 2016) when coupled to WUDAPT. It is therefore preferable, when simulations focusing on developing a concrete action plan for a given city are conducted, to use the detailed inputs from WUDAPT. Nevertheless, WUDAPT input is only available for Chicago among the metropolitan regions in this study. The dataset is under development and will need the participation of global researchers to make it available more broadly.

Acknowledgments

This work was supported by the U.S. National Science Foundation under Grant 1664091 and through the UWIN Sustainability Research Network Cooperative Agreement 1444758. The simulations were performed on the supercomputing clusters of the National Center for Atmospheric Research through projects UPRI0007 and UPRI0016.

Appendix A. Supplementary data

Supplementary data to this article can be found online at https://doi.org/10.1016/j.landurbplan.2019.02.004.

References

Bass, B., Krayenhoff, S., Martilli, A., & Stull, R. (2002). *Mitigating the urban heat island with green roof infrastructure.* Toronto: Urban Heat Island Summit.

Bowler, D. E., Buyung-Ali, L., Knight, T. M., & Pullin, A. S. (2010). Urban greening to cool towns and cities: A systematic review of the empirical evidence. *Landscape and Urban Planning, 97*(3), 147–155.

Brousse, O., Martilli, A., Foley, M., Mills, G., & Bechtel, B. (2016). WUDAPT, an efficient land use producing data tool for mesoscale models? Integration of urban LCZ in WRF over Madrid. *Urban Climate, 17*, 116–134.

Carter, T., & Fowler, L. (2008). Establishing green roof infrastructure through environmental policy instruments. *Environmental Management, 42*(1), 151–164.

Chen, F., Kusaka, H., Bornstein, R., Ching, J., Grimmond, C., Grossman-Clarke, S., ... Miao, S. (2011). The integrated WRF/urban modelling system: Development, evaluation, and applications to urban environmental problems. *International Journal of Climatology, 31*(2), 273–288.

Ching, J., Mills, G., Bechtel, B., See, L., Feddema, J., Wang, X., ... Mouzourides, P. (2018). World Urban Database and Access Portal Tools (WUDAPT), an urban weather, climate and environmental modeling infrastructure for the Anthropocene. *Bulletin of the American Meteorological Society*. https://doi.org/10.1175/BAMS-D-16-0236.1.

City of Chicago, 2009, Chicago Climate Action Plan:1-60.

City of Phoenix, 2016, 2015-2016 Sustainability Report:1-9.

City of Pittsburgh, 2017, Climate Action Plan Version 3.0:1-101.

County of Los Angeles, Department of Regional Planning, 2015, Unincorporated Los Angeles County Community Climate Action Plan:1-180.

de Munck, C., Pigeon, G., Masson, V., Meunier, F., Bousquet, P., Tréméac, B., ... Marchadier, C. (2013). How much can air conditioning increase air temperatures for a city like Paris, France? *International Journal of Climatology, 33*(1), 210–227.

Doick, K. J., Peace, A., & Hutchings, T. R. (2014). The role of one large greenspace in mitigating London's nocturnal urban heat island. *Science of the Total Environment, 493*, 662–671.

Drummond, W. J. (2010). Statehouse versus greenhouse: Have state-level climate action planners and policy entrepreneurs reduced greenhouse gas emissions? *Journal of the American Planning Association, 76*(4), 413–433.

Freitas, E. D., Rozoff, C. M., Cotton, W. R., & Dias, P. L. S. (2007). Interactions of an urban heat island and sea-breeze circulations during winter over the metropolitan area of São Paulo, Brazil. *Boundary-layer Meteorology, 122*, 43–65.

Gartland, L. M. (2012). *Heat islands: Understanding and mitigating heat in urban areas.* Routledge.

Georgescu, M., Morefield, P. E., Bierwagen, B. G., & Weaver, C. P. (2014). Urban adaptation can roll back warming of emerging megapolitan regions. *Proceedings of the National Academy of Sciences, 111*(8), 2909–2914.

Grimm, N. B., Faeth, S. H., Golubiewski, N. E., Redman, C. L., Wu, J., Bai, X., & Briggs, J. M. (2008). Global change and the ecology of cities. *Science, 319*(5864), 756–760.

Grimmond, S. (2007). Urbanization and global environmental change: Local effects of urban warming. *The Geographical Journal, 173*(1), 83–88.

Homer, C., Dewitz, J., Yang, L., Jin, S., Danielson, P., Xian, G., ... Megown, K. (2015). Completion of the 2011 National Land Cover Database for the conterminous United States–representing a decade of land cover change information. *Photogrammetric Engineering & Remote Sensing, 81*(5), 345–354.

Intergovernmental Panel on Climate Change (2014). *Climate change 2014–impacts: Regional Aspects.* Adaptation and Vulnerability: Cambridge University Press.

Jin, M., & Dickinson, R. E. (2010). Land surface skin temperature climatology: Benefitting from the strengths of satellite observations. *Environmental Research Letters, 5*(4), 044004.

Kim, Y. H., & Baik, J. J. (2005). Spatial and temporal structure of the urban heat island in Seoul. *Journal of Applied Meteorology, 44*(5), 591–605.

Li, D., Bou-Zeid, E., & Oppenheimer, M. (2014). The effectiveness of cool and green roofs as urban heat island mitigation strategies. *Environmental Research Letters, 9*(5), 055002.

Li, D., Bou-Zeid, E., Barlage, M., Chen, F., & Smith, J. A. (2013). Development and evaluation of a mosaic approach in the WRF-Noah framework. *Journal of Geophysical Research: Atmospheres, 118*(21).

Li, X., Zhou, W., Ouyang, Z., Xu, W., & Zheng, H. (2012). Spatial pattern of greenspace affects land surface temperature: Evidence from the heavily urbanized Beijing metropolitan area, China. *Landscape Ecology, 27*(6), 887–898.

Mackey, C. W., Lee, X., & Smith, R. B. (2012). Remotely sensing the cooling effects of city scale efforts to reduce urban heat island. *Building and Environment, 49*, 348–358.

Maimaitiyiming, M., Ghulam, A., Tiyip, T., Pla, F., Latorre-Carmona, P., Halik, Ü., ... Caetano, M. (2014). Effects of green space spatial pattern on land surface temperature: Implications for sustainable urban planning and climate change adaptation. *ISPRS Journal of Photogrammetry and Remote Sensing, 89*, 59–66.

Martilli, A., Clappier, A., & Rotach, M. W. (2002). An urban surface exchange parameterisation for mesoscale models. *Boundary-layer Meteorology, 104*(2), 261–304.

McCarthy, M. P., Best, M. J., & Betts, R. A. (2010). Climate change in cities due to global warming and urban effects. *Geophysical Research Letters, 37*(9) GL042845.

Miami-Dade County, 2010, GreenPrint: Our Design for a Sustainable Future:1-200.

Millstein, D., & Menon, S. (2011). Regional climate consequences of large-scale cool roof and photovoltaic arraydeployment. *Environmental Research Letters, 6*(3), 034001.

Morris, C. J. G., Simmonds, I., & Plummer, N. (2001). Quantification of the influences of wind and cloud on the nocturnal urban heat island of a large city. *Journal of Applied Meteorology, 40*(2), 169–182.

New York City, 2017, 1.5 °C: Aligning New York City with the Paris Climate Agreement 1-34.

Norton, B. A., Coutts, A. M., Livesley, S. J., Harris, R. J., Hunter, A. M., & Williams, N. S. (2015). Planning for cooler cities: A framework to prioritise green infrastructure to mitigate high temperatures in urban landscapes. *Landscape and Urban Planning, 134*, 127–138.

Oke, T. R. (1982). The energetic basis of the urban heat island. *Quarterly Journal of the Royal Meteorological Society, 108*(455), 1–24.

Parizotto, S., & Lamberts, R. (2011). Investigation of green roof thermal performance in temperate climate: A case study of an experimental building in Florianópolis city, Southern Brazil. *Energy and Buildings, 43*(7), 1712–1722.

Powers, J. G., Klemp, J. B., Skamarock, W. C., Davis, C. A., Dudhia, J., Gill, D. O., ... Grell, G. A. (2017). The weather research and forecasting model: Overview, system efforts, and future directions. *Bulletin of the American Meteorological Society, 98*(8), 1717–1737.

Ramamurthy, P., Li, D., & Bou-Zeid, E. (2017). High-resolution simulation of heatwave events in New York City. *Theoretical and Applied Climatology, 128*(1–2), 89–102.

Ramamurthy, P., Sun, T., Rule, K., & Bou-Zeid, E. (2015). The joint influence of albedo and insulation on roof performance: A modeling study. *Energy and Buildings, 102*, 317–327.

Reckien, D., Flacke, J., Dawson, R., Heidrich, O., Olazabal, M., Foley, A., ... Hurtado, S. D. G. (2014). Climate change response in Europe: What's the reality? Analysis of adaptation and mitigation plans from 200 urban areas in 11 countries. *Climatic Change, 122*(1–2), 331–340.

Rizwan, A. M., Dennis, L. Y., & Chunho, L. (2008). A review on the generation, determination and mitigation of Urban Heat Island. *Journal of Environmental Sciences, 20*(1), 120–128.

Sailor, D. J., Elley, T. B., & Gibson, M. (2012). Exploring the building energy impacts of green roof design decisions–a modeling study of buildings in four distinct climates. *Journal of Building Physics, 35*(4), 372–391.

Salamanca, F., Krpo, A., Martilli, A., & Clappier, A. (2010). A new building energy model coupled with an urban canopy parameterization for urban climate simulations—part I. formulation, verification, and sensitivity analysis of the model. *Theoretical and Applied Climatology, 99*(3), 331–344.

Salamanca, F., Georgescu, M., Mahalov, A., Moustaoui, M., & Wang, M. (2014).

Anthropogenic heating of the urban environment due to air conditioning. *Journal of Geophysical Research: Atmospheres, 119*(10), 5949–5965.
Santamouris, M. (2013). Using cool pavements as a mitigation strategy to fight urban heat island—A review of the actual developments. *Renewable and Sustainable Energy Reviews, 26*, 224–240.
Santamouris, M. (2014). Cooling the cities–a review of reflective and green roof mitigation technologies to fight heat island and improve comfort in urban environments. *Solar Energy, 103*, 682–703.
Sharma, A., Conry, P., Fernando, H., Hamlet, A. F., Hellmann, J., & Chen, F. (2016). Green and cool roofs to mitigate urban heat island effects in the Chicago metropolitan area: Evaluation with a regional climate model. *Environmental Research Letters, 11*(6), 64004.
Shen, H., Tan, H., & Tzempelikos, A. (2011). The effect of reflective coatings on building surface temperatures, indoor environment and energy consumption—An experimental study. *Energy and Buildings, 43*(2), 573–580.
Solcerova, A., van de Ven, F., Wang, M., Rijsdijk, M., & van de Giesen, N. (2017). Do green roofs cool the air? *Building and Environment, 111*, 249–255.
Speak, A. F., Rothwell, J. J., Lindley, S. J., & Smith, C. L. (2013). Reduction of the urban cooling effects of an intensive green roof due to vegetation damage. *Urban Climate, 3*, 40–55.
Steeneveld, G. J., Koopmans, S., Heusinkveld, B. G., Van Hove, L. W. A., & Holtslag, A. A. M. (2011). Quantifying urban heat island effects and human comfort for cities of variable size and urban morphology in the Netherlands. *Journal of Geophysical Research: Atmospheres, 116*, D20129.
Stewart, I. D., & Oke, T. R. (2012). Local climate zones for urban temperature studies. *Bulletin of the American Meteorological Society, 93*(12), 1879–1900.
Sun, T., Bou-Zeid, E., Wang, Z.-H., Zerba, E., & Ni, G.-H. (2013). Hydrometeorological determinants of green roof performance via a vertically-resolved model for heat and water transport. *Building and Environment, 60*, 211–224.
Takebayashi, H., & Moriyama, M. (2007). Surface heat budget on green roof and high reflection roof for mitigation of urban heat island. *Building and Environment, 42*(8), 2971–2979.
Wang, Z.-H., Fan, C., Myint, S. W., & Wang, C. (2016). Size Matters: What Are the Characteristic Source Areas for Urban Planning Strategies? *PLoS One, 11*(11), e0165726.
Wang, Z. H., Bou-Zeid, E., & Smith, J. A. (2013). A coupled energy transport and hydrological model for urban canopies evaluated using a wireless sensor network. *Quarterly Journal of the Royal Meteorological Society, 139*(675), 1643–1657.
Yang, J., & Wang, Z.-H. (2017). Planning for a sustainable desert city: The potential water buffering capacity of urban green infrastructure. *Landscape and Urban Planning, 167*, 339–347.
Yang, J., Wang, Z.-H., Chen, F., Miao, S., Tewari, M., Voogt, J. A., & Myint, S. (2015). Enhancing hydrologic modelling in the coupled weather research and forecasting–urban modelling system. *Boundary-Layer Meteorology, 155*(1), 87–109.
Yang, J., Wang, Z.-H., Georgescu, M., Chen, F., & Tewari, M. (2016). Assessing the impact of enhanced hydrological processes on urban hydrometeorology with application to two cities in contrasting climates. *Journal of Hydrometeorology, 17*(4), 1031–1047.
Yang, J., Wang, Z.-H., & Kaloush, K. E. (2015). Environmental impacts of reflective materials: Is high albedo a 'silver bullet' for mitigating urban heat island? *Renewable and Sustainable Energy Reviews, 47*, 830–843.
Yang, J., Wang, Z.-H., Kaloush, K. E., & Dylla, H. (2016). Effect of pavement thermal properties on mitigating urban heat islands: A multi-scale modeling case study in Phoenix. *Building and Environment, 108*, 110–121.
Yuan, C., & Chen, L. (2011). Mitigating urban heat island effects in high-density cities based on sky view factor and urban morphological understanding: A study of Hong Kong. *Architectural Science Review, 54*(4), 305–315.
Zinzi, M., & Agnoli, S. (2012). Cool and green roofs. An energy and comfort comparison between passive cooling and mitigation urban heat island techniques for residential buildings in the Mediterranean region. *Energy and Buildings, 55*, 66–76.